https://doi.org/10.5194/nhess-2019-349
Preprint. Discussion started: 13 December 2019

Natural Hazards and Earth System Sciences
Discussions

A multivariate statistical method for susceptibility analysis of the debris flow in Southwest China

Feng Ji[1], Zili Dai[2,*]

[1]State Key Laboratory of Geohazard Prevention and Geoenvironment Protection, Chengdu University of Technology, Chengdu 610059, China.

[2]Center for Natural Disaster Reduction Research and Education, Shimane University, 1060 Nishikawatsu-cho, Matsue, Shimane 690-8504, Japan.

[*]Corresponding Author: 87zili.dai@gmail.com.

Abstract: Southwest China is characterized by many steep mountains and deep valleys due to the uplift activity of the Tibetan Plateau. The 2008 Wenchuan Earthquake left large amounts of loose materials in this area, making it a severe disaster zone in terms of debris flow. Susceptibility is a significant factor of debris flow for evaluating its formation and impact. Therefore, it is in urgent need to analyze the susceptibility of debris flows in this area. At present, the susceptibility analysis models of the debris flow in Southwest China is mainly based on qualitative methods. Little quantitative prediction model is found in the literatures. This study evaluates 70 typical debris flow gullies as statistical samples, which are distributed along the Brahmaputra River, Nujiang River, Yalong River, Dadu River, and Ming River respectively. Nine indexes are chosen to construct a factor index system and then to evaluate the susceptibility of debris flow. They are the catchment area, longitudinal grade, average gradient of the slope on both sides of the gully, catchment morphology, valley slope orientation, loose material reserves, location of the main loose material, antecedent precipitation, and rainfall intensity. Then, an empirical model based on the quantification theory type I is established for the susceptibility prediction of debris flows in Southwest China. Finally, 10 debris flow gullies on the upstream of the Dadu River are analyzed to verify the reliability of the proposed model. The results show that the accuracy of the statistical model is 90%.

Keywords: Debris flow, susceptibility, prediction model, factor index system, multivariate statistical method.

https://doi.org/10.5194/nhess-2019-349
Preprint. Discussion started: 13 December 2019

1 Introduction

Debris flows are a common geological hazard in mountainous areas, which transport large amounts of sediment down-slope and cause serious damage to dwellings, roads, and other lifelines. China has mainly mountainous topography and is one of the most debris-flow prone countries in the world. Until March 2019, there are approximately 50,000 debris flows have occurred in China (Di et al. 2019). A significant percentage of these debris flows are distributed in Southwest China, particularly in the Wenchuan earthquake area, where large amounts of loose material were produced by the earthquake-induced landslides (Huang et al. 2015; Dai et al. 2017).

Due to the complex nature of debris flows, it is quite difficult to fully understand their initiation mechanism and precisely forecast their occurrence (Takahashi and Das, 2014). The uncertainty of debris flows poses significant threats to human lives in downstream areas (Schürch et al. 2011). Debris flow susceptibility expresses the occurrence possibility of debris flow in an area with respect to its geomorphologic characteristics (Kappes et al. 2011; Bertrand et al. 2013). Therefore, susceptibility analysis is an essential step to conduct the risk assessment of debris flow hazards. (Di et al. 2019; Zou et al. 2019).

Debris flow susceptibility analyses include two steps: 1) identification of the potential source areas and 2) prediction of the possible deposition areas (Kang and Lee, 2018). In the literature, a large number of prediction models have been proposed for the susceptibility analyses of debris flows. For the first step, statistical models that use various environmental factors contributing to possible instabilities are well-established. For example, Guinau et al. (2007) used a bivariate statistical procedure to carry out a terrain failure susceptibility analysis on debris flows that occurred in Nicaragua. Blahut et al. (2010) performed susceptibility assessment for the source areas of landslide induced debris flows in the Valtellina Valley based on bivariate statistics. Bertrand et al. (2013) performed two multivariate statistical models, a linear discriminant analysis (LDA) and a logistic regression (LR), to analyze the debris flow susceptibility of upland catchments. Jomelli et al. (2015) proposed a Bayesian hierarchical probabilistic model to investigate how debris flows respond to environmental and climatic variables in the French Alps. Carrara et al. (2008) discussed the application of different statistical models to debris flows in Val di Fassa, Trento Province. Lucà et al. (2011) compare bivariate and multivariate statistical models for the evaluation of gullying susceptibility in Northern Calabria, South Italy, and concluded that multivariate statistical

https://doi.org/10.5194/nhess-2019-349
Preprint. Discussion started: 13 December 2019

models were found to be the best model in predicting debris flow susceptibility of the study area. For the second step, the concept "angle of reach" was widely used in the empirical models to predict the runout distance of the debris flows (Scheidl and Rickenmann, 2010; Hürlimann et al. 2012; Horton et al. 2013). Recently, many numerical models were proposed to simulate the propagation of the debris flows and predict the deposition area. For example, Pirulli and Sorbino (2008) analyzed the propagation of potential debris flows in Southern Italy using two numerical codes RASH3D and FLO2D. Beguería et al. (2009) proposed a two-dimensional model based on numerical integration of the depth-averaged motion equations to predict the debris flow propagation over complex terrain near Lienz, Eastern Tyrol, Austria. Huang et al. (2015) presented a numerical model based on the smoothed particle hydrodynamic (SPH) method to calculate the runout distance of catastrophic debris flows that occurred in the Wenchuan Earthquake area. Gregoretti et al. (2016) used a cell model to simulate a debris flow that occurred on the Rio Lazer. Moradi et al. (2017) performed debris flow susceptibility zoning of debris flows in the Province of Reggio Calabria based on the SPH method. Some recent analysis methods of debris-flow susceptibility could be found in Cama et al. (2017), Prieto et al. (2018), and Rosatti et al. (2018).

The previous studies mentioned above have attempted to conduct debris flow susceptibility analysis in specified regions. Southwest China is characterized by steep mountains and deep valleys, and is strongly affected by the uplift activity of the Tibetan Plateau. Moreover, Southwest China has abundant loose material after the 2008 Wenchuan Earthquake. Therefore, a series of large-scale debris flows have been occurred during the rainy seasons in Southwestern China (Wu et al. 2019). At present, the susceptibility analysis of the debris flow in this area is mainly investigated based on qualitative methods with relevant specifications (Xu et al. 2013; Di et al. 2019). This work aims at providing a multivariate statistical method for susceptibility analysis of the debris flow in Southwest China. 70 debris flow gullies in Southwest China were analyzed, and nine key indicators were extracted through the initial analysis of the debris flows. Through multivariate statistics, an empirical formula of susceptibility was established, which was then validated with 10 debris flow gullies on the upstream of the Dadu River. It is worth noting that this work confines to identify the potential debris-flow source areas in Southwestern China, neglecting the runout of the phenomena.

https://doi.org/10.5194/nhess-2019-349
Preprint. Discussion started: 13 December 2019

Natural Hazards and Earth System Sciences
Open Access
Discussions

2 Study area characteristics of debris flow

Southwest China is charactered by steep mountains and deep valleys and is strongly affected by the uplift activity of the Qinghai–Tibet Plateau. Furthermore, there is abundant loose material and rainfall in this area. Therefore, it is a severe disaster zone in terms of debris flow. In the past three years, 70 typical debris flows distributed along the Brahmaputra River, Nujiang River, Yalong River, Dadu River, and Ming River are investigated. The location of the debris flows is shown in Figure 1. The formation condition of these debris flows in deep valley zones are analyzed, and a prediction assessment model for debris flow susceptibility is established based on a multivariate statistical method. The characteristics of the research area are summarized as follows.

In the upstream of the Brahmaputra River, 18 debris flows along the Dagu River and Jiexu River reaches are investigated. The lithology in this area is the irruptive rock of the late Yanshanian–Himalayan epoch, with a wide distribution of granodiorite. The average annual rainfall in this area is about 540 mm and concentrates mostly in summer. Large-scale ice-melting-type debris flow once occurred in this region. However, in recent years, the debris flows in this area are mainly caused by precipitation. Material reserves are abundant in the valleys, whereas unstable materials are found less frequently and the deposit zone is small. It is found that most of the debris flows in this area are in the decline phase, and most debris flow gullies are in the low-frequency category.

In the midstream of the Nujiang River catchment, 11 debris flow gullies located in the Zuogong River section are investigated. The stratum mainly includes the Permian Nacuo group slate and Triassic Wapu group marble. As this region is located in the subtropical zone south of the Himalayas, it is characterized by a humid climate and plentiful precipitation. This leads to an extensive distribution of debris flow gullies. In the midstream of the Yalong River catchment, 27 debris flow valleys are investigated, which belong to a plateau climate zone with complex meteorological and hydrological conditions. The concentricity and suddenness of rainfall provide hydraulic conditions for the debris flow breakouts. Collapses and landslides in the valley occur frequently. Moreover, the debris flow activity is intensified by unreasonable human engineering activities such as deforestation and accumulation of highway waste residues.

In the Dadu River catchment, 42 gullies in the midstream and the upstream are surveyed. This area is characterized by intense new tectonic movement, high earthquake intensity, and rock fragmentation on the mountain surface. Debris flow, collapse, and other geological disasters are widely distributed, and the deposit

https://doi.org/10.5194/nhess-2019-349
Preprint. Discussion started: 13 December 2019

zone of the debris flow is large. The maturity of the valley is high.

In the Minjiang River catchment, the Wenchuan River section are surveyed, and 32 debris flows are investigated. This region is characterized by abundant loose materials, frequent debris flows, and high possibility of the breakout of large-scale debris flows. Most of these debris flows are intensive in activity, occur very frequently, and have not declined in recent times.

3 Methodology

3.1 Investigation and statistical data

In total 70 debris flow gullies distributed in five water catchments in Southwestern China are investigated from the gully outlet to the watershed over the past three years. This work includes the investigation of the watershed terrain, geological structure, outbreak scale, loose material distribution, processes of occurrence and movement, frequency of debris flows, and so on. The role of each factor causing instability of the source materials are investigated. In addition, the precipitation data before the outbreak of debris flows are collected from local meteorological bureaus. The impulse force, sediment discharge, and other dynamic parameters are calculated.

3.2 Field test

All of the 70 debris flow gullies are traced, and bulk density tests (size 50 cm × 50 cm × 50 cm) and screening tests of the loose material are conducted on the deposit zone to determine the composition of debris flow sources. Besides, according to the superelevation and flow depth of the curved gully zone, the speed of the debris flow is estimated to provide the basic data for the dynamic parameter calculation.

3.3 Drilling and geophysical prospecting

For the active debris flow gullies, the geologic condition is complex. Considerable resources are invested in drilling and geophysical prospecting to obtain the volume, material composition, structure, and content of the fine-grained soil precisely.

3.4 Statistical technique

The statistical techniques can be grouped into bivariate and multivariate methods. A bivariate statistical

https://doi.org/10.5194/nhess-2019-349
Preprint. Discussion started: 13 December 2019

method analyses each parameter individually, therefore the calculation and application in bivariate statistical models are straightforward and efficient (Suzen and Doyuran, 2004). On the other hand, a multivariate statistical method considers the interaction of all parameters in controlling the occurrence of a phenomenon, and is considered as one of the best methods in predicting debris flow susceptibility (Lucà et al. 2011). Hayashi's quantification theory is a well-known multivariate statistical method developed by Hayashi (1961). It is widely used in various fields, such as risk assessment (Zhang et al. 2003; Jiang et al. 2010), psychological analysis (Sato et al. 1994), sociological surveys (Li et al. 2011; Han, 2014), and financial statistics (Choi et al. 2009). In this method, the qualitative and quantitative variables could be mutually transformed based on a reasonable principle. Therefore, this method has very good applicability to process the quantitative and qualitative influencing factors of debris flow risk.

Qualitative variables are termed items in quantification theory. All possibilities for each item are termed categories. A dummy variable $\delta_i(j, k)$ is introduced in the model to express the response of an item and the category for each sample:

$$\delta_i(j,k)=\begin{cases}1, & \text{if response of } i\text{th sample in the category } k \text{ of} \\ & \text{item } j \text{ to the corresponding external criterion;} \\ 0, & \text{otherwise.}\end{cases}\quad \begin{cases}i=1,2,\ldots, n;\\ j=1,2,\ldots, m.\end{cases} \tag{1}$$

where n is the number of samples and m denotes the number of items.

The response matrix X can be expressed as a $n \times p$-order matrix composed of all categories $\delta_i(j, k)$:

$$X=\begin{pmatrix}\delta_1(1,1)\cdots\delta_1(1,r_1) & \delta_1(2,1)\cdots\delta_1(2,r_2)\cdots\delta_1(m,1)\cdots\delta_1(m,r_m)\\ \delta_2(1,1)\cdots\delta_2(1,r_1) & \delta_2(2,1)\cdots\delta_2(2,r_2)\cdots\delta_2(m,1)\cdots\delta_2(m,r_m)\\ \vdots \quad\quad \vdots & \vdots \quad\quad \vdots \quad\quad \vdots \quad\quad \vdots\\ \delta_n(1,1)\cdots\delta_n(1,r_1) & \delta_n(2,1)\cdots\delta_n(2,r_2)\cdots\delta_n(m,1)\cdots\delta_n(m,r_m)\end{pmatrix} \tag{2}$$

To establish a quantitative analysis model, the qualitative and quantitative in-situ observations are used to fit the linear relationship between the concerned independent variable and the dependent variable. In the Hayashi's quantification theory, the random variable changes with the m variables:

$$y_i=\sum_{j=1}^{m}\sum_{k=1}^{r_j}\delta_i(j,k)b_{jk}+\varepsilon_i,\quad i=1,2,...,n \tag{3}$$

https://doi.org/10.5194/nhess-2019-349
Preprint. Discussion started: 13 December 2019

where y_i represents the susceptibility of the ith debris flow gully. r_j is the number of categories of the item j. b_{jk} is a constant coefficient depending on category k in item j. ε_i is a random error.

To establish an analysis model of debris flow susceptibility, some necessary steps should be followed based on Hayashi's quantification theory: 1) building an index system; 2) selecting samples and assigning values; 3) establishing the analysis model using single slopes; 4) conducting a significance test of the regression equation and each variable, 5) applying this analysis model to regional debris flow hazards evaluation.

4 Model generation and results

4.1 Indexes and categories in the statistical model

Considering the debris flow features and index-acquisition conditions, nine indexes are selected in this work to evaluate the susceptibility of debris flow gullies in Southwestern China, as listed in Table 1. They are the catchment area, longitudinal grade, average gradient of slope on both sides of the gully, catchment morphology, valley slope orientation, loose material reserves, loose material position, antecedent precipitation, and H_{1p} rainfall intensity. Each factor is classified into certain categories according to the values shown in Table 2.

4.2 Sample quantification

70 debris flow gullies in Southwest China are selected as the sample to evaluate the performance of the statistical model. The detail information of these debris flow gullies is listed in Table 3. The values of the samples are assigned according to Eq. 1, and the response from each category is obtained. The sample data then can be transformed into a "0-1" reflection matrix.

4.3 Statistical model based on Hayashi's quantification theory

When the quantitative theory and regression analysis take the binary-state variables 0 and 1, the equation can be revised as the following linear regression expression:

$$y_i = a_0 + \sum_{j=1}^{f} a_j x_{ij} + \varepsilon_i \quad (i = 1, ..., n) \tag{4}$$

https://doi.org/10.5194/nhess-2019-349
Preprint. Discussion started: 13 December 2019

Natural Hazards and Earth System Sciences
Open Access
EGU
Discussions

Based on Eq. 4 and matrix derivation regression calculation, the contribution values of each item are obtained, as shown in Table 4.

Substituting the numerical values in Eq. 4, the susceptibility prediction model of debris flow is established, which can be represented as follows:

$$\begin{aligned} Y = {} & 0.573x_{11} + 0.821x_{12} + 0.910x_{13} + 0.875x_{21} + 0.955x_{22} + 0.320x_{23} \\ & - 0.107x_{32} - 0.163x_{41} + 0.135x_{42} + 0.213x_{43} - 0.136x_{51} - 0.174x_{52} \\ & + 0.246x_{62} + 0.454x_{63} - 0.220x_{71} - 0.161x_{72} + 0.034x_{82} + 0.071x_{83} \\ & - 0.038x_{91} + 0.043x_{92} \end{aligned} \tag{5}$$

In Eq. 5, Y is the susceptibility for the debris flow. In the proposed model, the susceptibility values are classified into three categories. When the predicted value (Y) is less than 1.5, the susceptibility of the debris flow is considered as low. When Y is greater than or equal to 1.5 but less than 2.5, the susceptibility is medium. When Y is greater than or equal to 2.5, the susceptibility is high. The meanings of x_{11}, x_{12}, x_{13} and other indexes are detailed in Table 2 and 3.

5 Validation and discussion

5.1 Fitting degree analysis

Table 5 shows the regression coefficient of determination and the standard deviation. As the susceptibility of the debris flow is controlled by many factors, the coefficient of determination reaches 74.9%, reflecting a favorable level of fit.

5.2 Self-test coincidence rate

The values of each index are used in the established model to calculate the predicted values of the susceptibility, and then the predicted values are compared with the actual values (Fig. 2).

As shown in Fig. 2, the predicted values of debris-flow susceptibility are graded. When the predicted value (Y) is less than 1.5, the susceptibility to debris flow is low. When the predicted value (Y) is greater than or equal to 1.5 but less than 2.5, the susceptibility is medium. When the predicted value (Y) is greater than or equal to 2.5, the susceptibility is high.

From the prediction results (Table 6), the coincidence rate is 78.53% for low-susceptibility debris flow

https://doi.org/10.5194/nhess-2019-349
Preprint. Discussion started: 13 December 2019

Natural Hazards and Earth System Sciences
Discussions

valleys, 92.38% for medium-susceptibility debris flow valleys, 82.01% for high-susceptibility debris flow valleys, and 86.38% for all the samples, which indicates that the regression model can predict the debris-flow susceptibility well.

5.3 Residual error analysis

Figure 3 is a residual error distribution chart. It shows that the residual error fluctuates between ±0.45, which indicates that the regression line fits the observed values well. The residual error frequency approximates a normal distribution.

5.4 Verification of proposed model

The Kaka basin is located on the upper part of the Dadu River, southeast of the Qinghai–Tibet Plateau. The valley is deep and the river runs from north to south. The regional topography is characterized by high altitudes in the east and low altitudes in the west. The terrain is composed of high mountains with elevations of 2000 m. There are three layers of wide valley mesas, and the uplift of mountains and river erosion is significant. The river elevation in the Kaka basin is approximately 1800 m, the river width is 140–185 m, and the slope angle is approximately 45–60°. The main fractures are denoted as F_1, F_5, $F_{5\text{-}1}$, F_6, and F_7 in Fig. 4. The trend is NW, and they have a 40–60° angle with the river. A series of debris flow gullies have occurred in the basin.

10 typical debris flow gullies on the upstream of the Dadu River are selected as samples for the model validation (as shown in Fig. 5, and listed in Tab. 7). The accuracy of the established model is verified through the comparison with field investigation results. Table 8 provides the relevant basic data for the samples. Each secondary index is transformed into a 0-1 mode, and all the samples are adopted to construct a 9 × 26 matrix.

For the 10 verification samples, according to calculation results, the accuracy rate of the model is 90% (Tab. 8), indicating that the prediction model is applicable to the data.

6 Conclusions

Debris flows frequently occurred in Southwest China and resulted in severe damage to dwellings and lifelines. Based on the Hayashi's quantification theory, an initiation susceptibility model of debris flows in Southwest

https://doi.org/10.5194/nhess-2019-349
Preprint. Discussion started: 13 December 2019

China was proposed in this work. The following conclusions can be drawn:

1) According to the topography and geomorphology characteristics in Southwest China, the following nine indexes were used as evaluation factors of debris flow initiation susceptibility: the catchment area, longitudinal grade, average gradient of the slope on both sides of the gully, catchment morphology, valley slope orientation, loose material reserves, location of the main loose material, antecedent precipitation, and rainfall intensity.
2) 70 typical debris flow gullies distributed along the Brahmaputra River, Nujiang River, Yalong River, Dadu River, and Ming River were investigated as statistical samples. The parameters of the prediction model were obtained based on the Hayashi's quantitative theory and regression analysis.
3) The proposed model was applied to analyze the initiation susceptibility of 10 debris flow gullies located on the upstream of the Dadu River, and the result showed that the judgment coincidence rate is 90%, indicating that the proposed model can accurately predict the initiation susceptibility of debris flow gullies in Southwest China.

Acknowledgments:

The presented work was supported by the Sichuan Science and Technology Program (2018JY0471), and Sichuan Provincial Youth Science and Technology Innovation Team Special Projects of China (No. 2017TD0018), the Open Fund of Key Laboratory of Geological Hazards on Three Gorges Reservoir Area (China Three Gorges University) (2018KDZ01), Ministry of Education, and the JSPS Grant-in-Aid for Early Career Scientists (19K14804).

References

Beguería, S., Van Asch, T. W., Malet, J. P., and Gröndahl, S.: A GIS-based numerical model for simulating the kinematics of mud and debris flows over complex terrain, Natural Hazards and Earth System Sciences, 9(6), 1897–1909, 2009.

Bertrand, M., Liébault, F., and Piégay, H.: Debris-flow susceptibility of upland catchments, Natural Hazards, 67(2), 497–511, 2013.

Blahut, J., van Westen, C. J., and Sterlacchini, S.: Analysis of landslide inventories for accurate prediction of

https://doi.org/10.5194/nhess-2019-349
Preprint. Discussion started: 13 December 2019

debris-flow source areas, Geomorphology, 119(1–2), 36–51, 2010.

Cama, M.; Lombardo, L., Conoscenti, C., and Rotigliano, E.: Improving transferability strategies for debris flow susceptibility assessment: Application to the Saponara and Itala catchments (Messina, Italy), Geomorphology, 288, 52–65, 2017.

Carrara, A., Crosta, G., and Frattini, P.: Comparing models of debris-flow susceptibility in the alpine environment, Geomorphology, 94(3–4), 353–378, 2008.

Choi, J. Y., Lee, J. H., Sohn, S. Y.: Impact analysis for national R&D funding in science and technology using quantification method II. Research Policy, 38(10), 1534–1544, 2009.

Cui, P., Guo, X., Yan, Y., Li, Y., and Ge, Y.: Real-time observation of an active debris flow watershed in the Wenchuan Earthquake area, Geomorphology, 321, 153–166, 2018.

Dai, Z., Huang, Y., Cheng, H., and Xu, Q.: SPH model for fluid–structure interaction and its application to debris flow impact estimation, Landslides, 14(3), 917–928, 2017.

Di, B. F., Zhang, H. Y., Liu, Y. Y., Li, J. R., Chen, N. S., Stamatopoulos, C.A., Luo, Y.Z., Zhan, Y.: Assessing Susceptibility of Debris Flow in Southwest China Using Gradient Boosting Machine. Scientific Reports, 9: 12532, 2019.

Gregoretti, C., Degetto, M., and Boreggio, M.: GIS-based cell model for simulating debris flow runout on a fan, Journal of hydrology, 534, 326–340, 2016.

Guinau, M., Vilajosana, I., and Vilaplana, J. M.: GIS-based debris flow source and runout susceptibility assessment from DEM data? A case study in NW Nicaragua. Natural Hazards and Earth System Science, 7(6), 703–716, 2007.

Han, S. T.: Sensitivity analysis for ranked data. Journal of the Korean Statistical Society, 43(1), 1–9, 2014.

Hayashi, C.: Sample survey and theory of quantification. Bulletin of the international statistical institute, 38, 505–514, 1961.

Horton, P., Jaboyedoff, M., Rudaz, B. E. A., and Zimmermann, M.: Flow-R, a model for susceptibility mapping of debris flows and other gravitational hazards at a regional scale. Natural hazards and earth system sciences, 13(4), 869–885, 2013.

Huang, Y., Cheng, H., Dai, Z., Xu, Q., Liu, F., Sawada, K., Moriguchi, S., and Yashima, A. SPH-based numerical

https://doi.org/10.5194/nhess-2019-349
Preprint. Discussion started: 13 December 2019

simulation of catastrophic debris flows after the 2008 Wenchuan earthquake, Bulletin of Engineering Geology and the Environment, 74(4), 1137–1151, 2015.

Hürlimann, M., Abancó, C., and Moya, J.: Rockfalls detached from a lateral moraine during spring season. 2010 and 2011 events observed at the Rebaixader debris-flow monitoring site (Central Pyrenees, Spain), Landslides, 9(3), 385–393, 2012.

Jiang, Y., Wang, C., and Zhao, X.: Damage assessment of tunnels caused by the 2004 Mid Niigata Prefecture Earthquake using Hayashi's quantification theory type II, Natural hazards, 53(3), 425–441, 2010.

Jomelli, V., Pavlova, I., Eckert, N., Grancher, D., and Brunstein, D.: A new hierarchical Bayesian approach to analyse environmental and climatic influences on debris flow occurrence, Geomorphology, 250, 407–421, 2015.

Kang, S., Lee, S. R.: Debris flow susceptibility assessment based on an empirical approach in the central region of South Korea, Geomorphology, 308, 1–12, 2018.

Kappes, M. S., Malet, J. P., Remaître, A., Horton, P., Jaboyedoff, M., and Bell, R.: Assessment of debris-flow susceptibility at medium-scale in the Barcelonnette Basin, France, Natural Hazards and Earth System Sciences, 11(2), 627–641, 2011.

Li, Z., Munemoto, J., Yoshida, T.: Analysis of Behaviors along the Waterside in a Chinese Residential Quarter. Journal of Asian Architecture and Building Engineering, 10(1), 85–92, 2011.

Li, N., Gu, W., Okada, N., and Levy, J. K.: The utility of Hayashi's quantification theory for assessment of land surface indices in influence of dust storms: a case study in Inner Mongolia, China, Atmospheric Environment, 39(1), 119–126, 2005.

Lucà, F., Conforti, M., Robustelli, G.: Comparison of GIS-based gullying susceptibility mapping using bivariate and multivariate statistics: Northern Calabria, South Italy, Geomorphology, 134(3–4), 297–308, 2011.

Moraci, N., Mandaglio, M. C., Gioffrè, D., Pitasi, A.: Debris flow susceptibility zoning: an approach applied to a study area, Rivista Italiana di Geotecnica, 51(2), 47–62, 2017.

Prieto, J. A., Journeay, M., Acevedo, A. B., Arbelaez, J. D., and Ulmi, M.: Development of structural debris flow fragility curves (debris flow buildings resistance) using momentum flux rate as a hazard parameter, Engineering Geology, 239, 144–157, 2018.

Pirulli, M., and Sorbino, G.: Assessing potential debris flow runout: a comparison of two simulation models, Natural Hazards and Earth System Sciences, 8, 961–971, 2008.

Rosatti, G., Zorzi, N., Zugliani, D., Piffer, S., and Rizzi, A.: A Web Service ecosystem for high-quality, cost-effective debris-flow hazard assessment. Environmental modelling & software, 100, 33–47, 2018.

Sato, T., Sugawara, M., Toda, M., Shima, S., Kitamura, T.: Rearing related stress and depressive severity. Shinrigaku kenkyu: The Japanese journal of psychology, 64(6), 409–416, 1994.

Scheidl, C., and Rickenmann, D.: Empirical prediction of debris-flow mobility and deposition on fans, Earth Surface Processes and Landforms: The Journal of the British Geomorphological Research Group, 35(2), 157–173, 2010.

Schürch, P., Densmore, A. L., Rosser, N. J., and McArdell, B. W.: Dynamic controls on erosion and deposition on debris-flow fans. Geology, 39(9), 827–830, 2011.

Suzen, L. M., and Doyuran, V.: A comparison of the GIS based landslide susceptibility assessment methods: multivariate versus bivariate, Environmental Geology 45, 665–679, 2004.

Takahashi, T., and Das, D. K.: Debris flow: mechanics, prediction and countermeasures. CRC press, 2014.

Wu, S., Chen, J., Zhou, W., Iqbal, J., and Yao, L.: A modified Logit model for assessment and validation of debris-flow susceptibility, Bulletin of Engineering Geology and the Environment, 78(6), 4421–4438, 2019.

Xu, Q., Zhang, S., Li, W. L., and Van Asch, T. W.: The 13 August 2010 catastrophic debris flows after the 2008 Wenchuan earthquake, China, Natural Hazards and Earth System Sciences, 12, 201–216, 2012.

Xu, W., Yu, W., Jing, S., Zhang, G., and Huang, J.: Debris flow susceptibility assessment by GIS and information value model in a large-scale region, Sichuan Province (China), Natural hazards, 65(3), 1379–1392, 2013.

Zhang, X., Zhang, Z., and Peng, S.: Application of the second theory of quantification in identifying gushing water sources of coal mines, Journal of China university of mining and technology, 32(3), 251–254, 2003.

Zhao, F.C.: Chinese drainage map, China Atlas Press, 2014.

Zou, Q., Cui, P., He, J., Lei, Y., and Li, S.: Regional risk assessment of debris flows in China—An HRU-based approach, Geomorphology, 340, 84–102, 2019.

https://doi.org/10.5194/nhess-2019-349
Preprint. Discussion started: 13 December 2019

Natural Hazards and Earth System Sciences
Open Access
Discussions

List of Table Captions

https://doi.org/10.5194/nhess-2019-349
Preprint. Discussion started: 13 December 2019

Table 1 Nine indexes used in the prediction model of debris flow susceptibility

Symbol	Physical significance
x_1	Catchment area （km^2）
x_2	Longitudinal grade（‰）
x_3	Average gradient of slope on both sides of gully （°）
x_4	Catchment morphology
x_5	Valley slope orientation
x_6	Loose Material reserves （$10^4\,m^3/km^2$）
x_7	Main loose material position
x_8	Antecedent precipitation
x_9	H_{1p} rainfall intensity （mm）

Table 2 Assessment index system of the model and relative categories

Item	Category	value	Item	Category	Value
Catchment area x_1 (km²)	x_{11}	<1 km²	Valley slope orientation x_5	x_{51}	Sunny slope
	x_{12}	1–10 km²		x_{52}	Shady slope
	x_{13}	10–100 km²	Loose material reserves x_6 (10⁴ m³/km²)	x_{61}	<1 × 10⁴ m³/km²
	x_{14}	≥100 km²		x_{62}	1–5 × 10⁴ m³/km²
Longitudinal grade x_2 (‰)	x_{21}	<100‰		x_{63}	≥ 5×10⁴ m³/km²
	x_{22}	100‰–300‰	Main loose material position x_7	x_{71}	Upstream or tributary
	x_{23}	≥300‰		x_{72}	Middle and lower reaches
Average gradient of slope on both sides of gully x_3 (°)	x_{31}	<30		x_{73}	Toe of gully
	x_{32}	30–40°	Antecedent precipitation x_8	x_{81}	Inadequacy
	x_{33}	≥40°		x_{82}	Middle
Catchment morphology x_4	x_{41}	$Z < 0.3$		x_{83}	Middle
	x_{42}	$Z = 0.3–0.7$	H_{1p} rainfall intensity x_9 (mm)	x_{91}	< 30 mm
	x_{43}	$Z \geq 0.7$		x_{92}	≥ 30 mm

Note: Z is the length to width ratio of the di basin

https://doi.org/10.5194/nhess-2019-349
Preprint. Discussion started: 13 December 2019

Table 3 Sample data for debris flow examples from Southwest China

No.	x_1	x_2	x_3	x_4	x_5	x_6	x_7	x_8	x_9	**Susceptibility**
1	0.77	567	35	Long strip	SE	8.05	Upstream	Inadequacy	26.38	Low
2	13.3	366	28	Ellipse	SE	10.04	Upstream	Inadequacy	26.38	Medium
3	2.62	624	37	Long strip	SE	4.39	Upstream	Inadequacy	26.38	Low
4	2.47	624	36	Long strip	SE	26.06	Middle and lower reaches	Inadequacy	26.38	Low
5	71.64	194	22	Ellipse	S	8.06	Upstream	Inadequacy	26.38	Medium
6	18.89	344	35	Suborbicular	NE	3.08	Upstream	Inadequacy	26.38	Low
7	13.01	404	36	Ellipse	NW	3.43	Upstream	Inadequacy	26.38	Low
8	43.51	199	28	Suborbicular	NE	4.01	Upstream	Inadequacy	26.38	Medium
9	38.4	251	37	Long strip	SE	5.38	Upstream	Inadequacy	26.38	Medium
10	4.04	412.53	37	Long strip	NE	6.15	Upstream	Inadequacy	26.38	Low
11	1.39	480	35	Long strip	N	7.85	Upstream	Inadequacy	26.38	Low
12	1.62	569.4	36	Long strip	S	19.11	Middle and lower reaches	Inadequacy	26.38	Low
13	13.23	280.61	31	Ellipse	N	3.07	Middle and lower reaches	Inadequacy	26.38	Medium
14	2.48	536.68	41	Long strip	S	22.63	Upstream	Inadequacy	26.38	Low
15	5.15	507.69	39	Ellipse	S	10.74	Upstream	Inadequacy	26.38	Low
16	1.25	630.34	43	Suborbicular	NE	6.44	Middle and lower reaches	Inadequacy	26.38	Low
17	135.6	139.46	30	Suborbicular	NE	3.91	Upstream	Inadequacy	26.38	Low
18	53.42	169.87	30	Ellipse	SW	1.89	Middle and lower reaches	Fully	32.85	Medium
19	169.72	121.62	25	Ellipse	S	0.98	Branch trench、Upstream	Fully	32.85	Medium
20	15.53	171.2	36	Long strip	N	3.24	Upstream	Fully	32.85	Low
21	31.35	171	33	Ellipse	NE	2.74	Middle and lower reaches	Fully	32.85	High
22	7.37	462.11	35	Suborbicular	NE	7.06	Middle and lower reaches	Fully	32.85	High
23	20.99	235.79	25	Ellipse	SW	1.47	Upstream	Fully	32.85	Low

https://doi.org/10.5194/nhess-2019-349
Preprint. Discussion started: 13 December 2019

No.	x_1	x_2	x_3	x_4	x_5	x_6	x_7	x_8	x_9	Susceptibility
24	275.41	60	23	Ellipse	SE	0.89	Upstream	Fully	32.85	Low
25	211.4	94	34	Ellipse	NW	1.04	Tributary	Middle	32.85	Low
26	8.89	256	36	Long strip	SW	3.79	Upstream	Fully	32.85	Low
27	28.91	190	31	Ellipse	SE	2.20	Middle and lower reaches	Fully	32.85	Medium
28	34.84	158	43	Long strip	SW	0.90	Middle and lower reaches	Fully	42.2	Medium
29	102.7	110	29	Long strip	NE	0.75	Middle and lower reaches	Fully	42.2	Low
30	84.81	146.2	32	Ellipse	NE	0.78	Branch trench	Fully	42.2	Low
31	132.02	129.5	35	Ellipse	SW	0.42	Upstream	Fully	42.2	Medium
32	5.5	318.01	33	Ellipse	NE	6.37	Middle and lower reaches	Fully	42.2	Medium
33	124.3	117.9	26	Ellipse	SW	1.37	Branch trench, Upstream	Fully	42.2	Low
34	26.2	203.9	36	Ellipse	SE	3.85	Upstream	Fully	42.2	Medium
35	29.56	205.1	32	Long strip	SW	1.84	Upstream	Fully	42.2	Low
36	80.34	119.1	38	Long strip	NE	1.51	Branch trench, Upstream	Fully	42.2	Low
37	8.45	301.5	37	Ellipse	NE	2.06	Upstream	Fully	42.2	Medium
38	16.26	217.1	36	Long strip	SE	1.15	Branch trench, Upstream	Fully	42.2	Low
39	77.5	138.5	41	Long strip	NE	1.22	Upstream	Fully	42.2	Low
40	23.1	235.52	24	Long strip	SW	1.68	Upstream	Fully	42.2	Low
41	47.01	166	30	Ellipse	NE	1.69	Toe of gully	Fully	42.2	Medium
42	83.11	125	31	Ellipse	NE	0.40	Upstream	Fully	42.2	Low
43	21.11	238	32	Ellipse	SW	0.87	Upstream	Fully	42.2	Medium
44	73.11	156	32	Ellipse	SE	1.10	Middle and lower reaches	Middle	43.12	Medium
45	64.7	144	33	Ellipse	NW	0.78	Toe of gully	Middle	43.12	High
46	21.87	242.95	36	Ellipse	NW	1.55	Branch trench, Upstream	Middle	43.12	Low
47	3.5	530.4	42	Ellipse	NW	8.34	Middle and lower reaches	Middle	43.12	Medium

https://doi.org/10.5194/nhess-2019-349
Preprint. Discussion started: 13 December 2019

Natural Hazards and Earth System Sciences
Open Access
Discussions

No.	x_1	x_2	x_3	x_4	x_5	x_6	x_7	x_8	x_9	Susceptibility
48	26.66	296.6	33	Ellipse	SE	4.70	Middle and lower reaches	Middle	43.12	Medium
49	32.23	178.35	30	Suborbicular	S	5.91	Middle and lower reaches	Middle	28.47	Medium
50	40.03	164.6	31	Ellipse	SE	5.59	Middle and lower reaches	Middle	28.47	Medium
51	3.25	235.43	35	Ellipse	NW	2.18	Upstream	Middle	28.47	Low
52	351.2	92.4	24	Ellipse	S	10.37	Branch trench	Middle	28.47	Medium
53	8.85	220.35	36	Suborbicular	NW	4.01	Branch trench, Upstream	Middle	28.47	Low
54	25.31	203.62	30	Long strip	S	4.75	Middle and lower reaches	Middle	28.47	High
55	1.78	214.58	28	Suborbicular	NE	0.73	Upstream	Middle	28.47	Low
56	5.8	246.48	34	Ellipse	SW	15.79	Middle and lower reaches	Middle	28.47	High
57	7.6	230.09	42	Ellipse	S	17.34	Middle and lower reaches	Middle	28.47	Medium
58	1.7	140.37	36	Long strip	SE	136.82	Middle and lower reaches	Middle	28.47	Medium
59	53.27	132.43	32	Ellipse	SE	10.33	Upstream	Middle	28.47	Medium
60	14.15	178.6	28	Suborbicular	SW	55.50	Middle and lower reaches	Fully	41.1	High
61	1.48	244.2	33	Suborbicular	SW	32.81	Middle and lower reaches	Fully	41.1	High
62	0.89	256.8	38	Suborbicular	SW	18.81	Middle and lower reaches	Fully	41.1	Medium
63	0.98	243.2	35	Suborbicular	SW	12.70	Middle and lower reaches	Fully	41.1	Medium
64	3.73	120	24	Long strip	SW	9.51	Upstream	Fully	41.1	Medium
65	3.37	450.9	40	Ellipse	SE	8.80	Upstream	Fully	41.1	Medium
66	0.57	207.7	31	Suborbicular	SW	36.89	Middle and lower reaches	Fully	41.1	High
67	3.02	488.8	42	Ellipse	SE	20.99	Middle and lower reaches	Fully	41.1	High
68	7.59	352	28	Ellipse	NE	19.26	Middle and lower reaches	Fully	41.1	High
69	32.04	223	23	Ellipse	NW	13.67	Middle and lower reaches	Fully	41.1	High
70	3.27	235	35	Ellipse	NE	9.29	Upstream	Fully	41.1	Low

https://doi.org/10.5194/nhess-2019-349
Preprint. Discussion started: 13 December 2019

Natural Hazards and Earth System Sciences
Discussions

Table 4 Score values of each index after normalization

Item	Category	Value	Item	Category	Value
Catchment area x_1 (km^2)	x_{11}	0.573	Valley slope orientation x_5	x_{51}	-0.136
	x_{12}	0.821		x_{52}	-0.174
	x_{13}	0.910	Loose material reserves x_6 (10^4 m^3/km^2)	x_{61}	0
	x_{14}	0		x_{62}	0.246
Longitudinal grade x_2 (‰)	x_{21}	0.875		x_{63}	0.454
	x_{22}	0.955	Main loose material position x_7	x_{71}	-0.220
	x_{23}	0.320		x_{72}	-0.161
Average gradient of slope on both sides of gully x_3 (°)	x_{31}	0		x_{73}	0
	x_{32}	-0.107	Antecedent precipitation x_8	x_{81}	0
	x_{33}	0		x_{82}	0.034
Catchment morphology x_4	x_{41}	-0.163		x_{83}	0.071
	x_{42}	0.135	H_{1p} rainfall intensity x_9 (mm)	x_{91}	-0.038
	x_{43}	0.213		x_{92}	0.043

https://doi.org/10.5194/nhess-2019-349
Preprint. Discussion started: 13 December 2019

Table 5 Quantitative model eigenvalue

Model	*R*	R^2	Standard deviation
1	0.865	0.749	0.289

https://doi.org/10.5194/nhess-2019-349
Preprint. Discussion started: 13 December 2019

Natural Hazards and Earth System Sciences
Open Access
Discussions

Table 6 Prediction model accuracy

Category	Low	Medium	High
Accuracy (%)	78.53	92.38	82.01

https://doi.org/10.5194/nhess-2019-349
Preprint. Discussion started: 13 December 2019

Table 7 Sample data from Kaka area in the upstream of Dadu River

No.	Ditch name	x_1	x_2	x_3	x_4	x_5	x_6	x_7	x_8	x_9
1	Luotuo	227.1	102	25	0.745	SE	0.87	Middle and lower	Fully	43.8
2	Qiongshan	84.90	200	28	0.907	SE	10.67	Middle and lower	Fully	43.8
3	Shuikazi	49.78	209	31	0.534	SE	4.82	Middle and lower	Fully	43.8
4	Bawang	11.84	310	32	0.219	SW	2.36	Upstream	Middle	43.8
5	Shenluo	4.54	455	33	0.580	NW	42.46	Toe of gully	Middle	43.8
6	Mueryue	35.81	206	36	0.376	NW	10.08	Upstream	Fully	43.8
7	Sezu	4.23	613	42	0.812	NW	26.24	Middle and lower	Fully	43.8
8	Muerluo	11.93	358	34	0.546	NW	9.98	Upstream	Middle	43.8
9	Yaneryan	30.01	242	34	0.382	SW	5.64	Middle and lower	Middle	43.8
10	Linong	10.09	332	35	0.448	NW	24.30	Middle and lower	Middle	43.8

https://doi.org/10.5194/nhess-2019-349
Preprint. Discussion started: 13 December 2019

Natural Hazards and Earth System Sciences
Open Access
EGU
Discussions

Table 8 Comparison of predicted values and actual measured values

Number	**1**	**2**	**3**	**4**	**5**	**6**	**7**	**8**	**9**	**10**
Calculated Y value	2.562	1.805	1.764	2.540	2.748	2.167	1.705	1.843	1.348	2.421
Predicted susceptibility	High	Medium	Medium	High	High	Medium	Medium	Medium	Low	Medium
Geological judgment of actual susceptibility	High	Medium	Medium	High	High	Medium	Medium	Medium	Low	High
Accuracy	Right	Right	Right	Right	Right	Right	Right	Right	Right	**Wrong**

https://doi.org/10.5194/nhess-2019-349
Preprint. Discussion started: 13 December 2019

Natural Hazards and Earth System Sciences
Discussions

List of Figure Captions

https://doi.org/10.5194/nhess-2019-349
Preprint. Discussion started: 13 December 2019

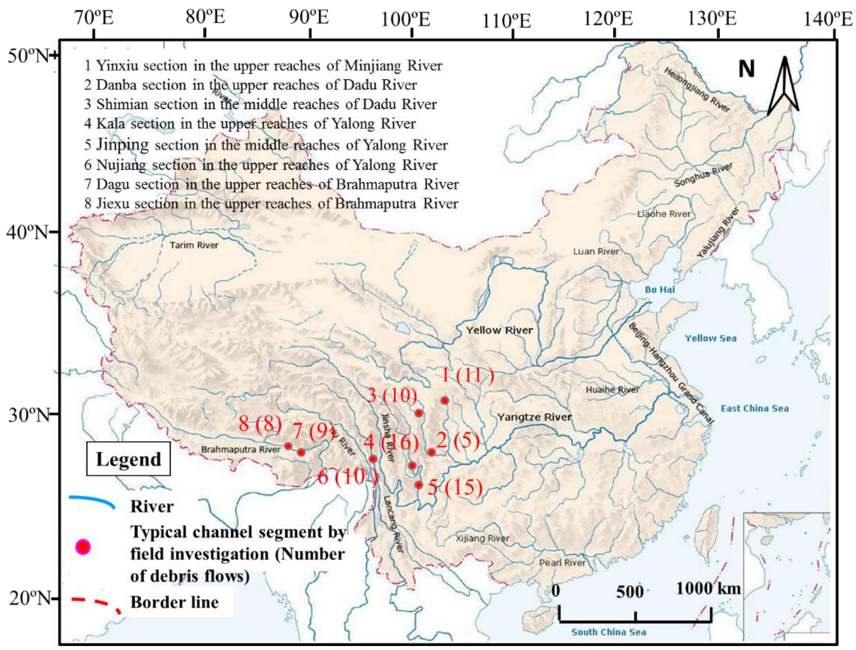

Fig.1 Distribution of the investigated debris flow gullies (the base map is from Zhao 2014)

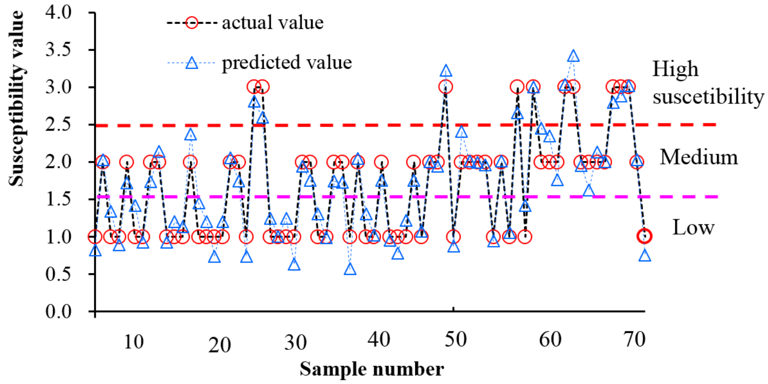

Fig.2 Comparison of measured and predicted values

https://doi.org/10.5194/nhess-2019-349
Preprint. Discussion started: 13 December 2019

Natural Hazards and Earth System Sciences
Discussions
Open Access

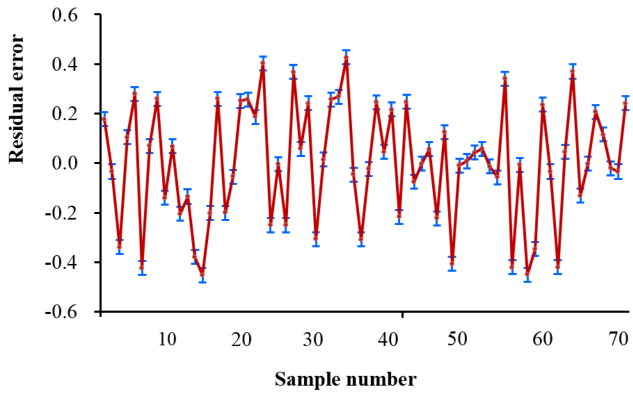

Fig.3 Residual distribution model of self-test standard value of susceptibility degree

https://doi.org/10.5194/nhess-2019-349
Preprint. Discussion started: 13 December 2019

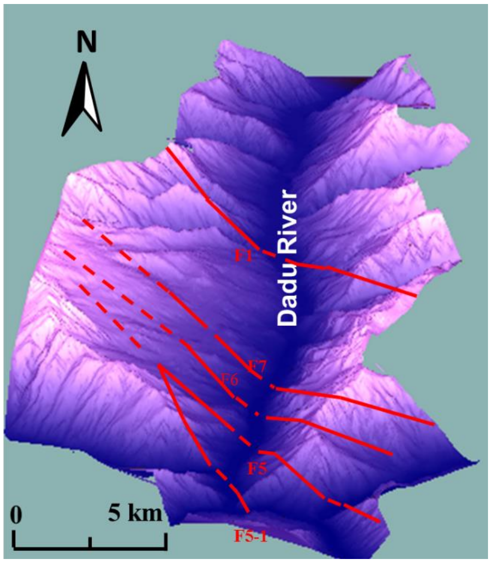

Fig.4 Kaka basin geomorphology of Dadu River

https://doi.org/10.5194/nhess-2019-349
Preprint. Discussion started: 13 December 2019

Natural Hazards and Earth System Sciences
Open Access
Discussions

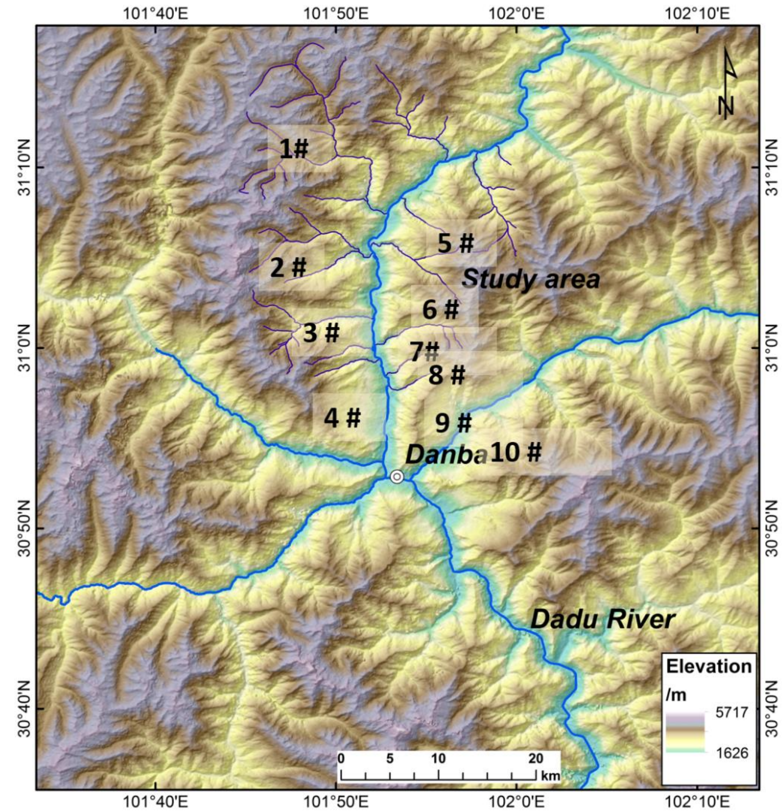

Fig.5 Debris flow gullies on both sides of Dadu River